

Power density of spinel cathode secondary lithium-ion batteries

A.M. Wilson^{*}, Jan N. Reimers

NEC Moli Energy (Canada), 20,000 Stewart Crescent, Maple Ridge, BC, Canada

Abstract

Several commonly used representations of power densities and their shortcomings for describing the high-power, short-pulse regime are discussed. The Specific Power Profile (SPP) is presented as an informative and well-defined power density representation. The power densities of Mn-based and Co-based Li-ion (commercially available MOLICEL), nickel cadmium, and nickel metal hydride cells are compared using the SPP. © 1999 Elsevier Science S.A. All rights reserved.

Keywords: Cell; Power density; Voltage

1. Introduction

The power density (W/kg) of a battery is determined by a number of factors such as cell temperature, lower cutoff voltage, state of charge and, most notably, the time scale of application under consideration. For example, batteries can generally deliver much higher sustained power for 1 s then they can deliver for 100 s.

Here we mention, briefly, some of the more popular methods used to represent power densities and why we feel that they are not adequate for high-power applications, like electric vehicles and power tools.

The most common representations of battery power densities consist of a single number, arrived at by applying specific voltage and time restrictions [1,2]. Although these restrictions are usually chosen with a particular application in mind, they can also be chosen in a regime which is favorable to a specific technology. Unfortunately, the specific method is often not mentioned [2].

One common method for determining a single-value power density is by first selecting a lower voltage cutoff (V_{LCV}) and time limit (t_{LCV}). Then, the current which results in the cell being discharged to V_{LCV} after t_{LCV} has elapsed (i.e., I_{LCV} such that $V(I_{LCV}, t_{LCV}) = V_{LCV}$) is used to calculate a single number for the power density ($= V_{LCV} \times I_{LCV} / M_{CELL}$, where M_{CELL} is the cell mass).

The United States Advanced Battery Consortium (USABC) has a fairly complex and well-defined criteria by

which to determine a power density of a cell [1]. Four different equations are used to calculate power densities, and the minimum of them is chosen to represent the peak power of the cell. While this method may provide a useful power density metric for the USABC (as it was only intended to do), it does not give information which may be useful to other applications.

Another common method plots the current or power density vs. the ‘service time’ or ‘hours of service’ [2]. While this appears to be a useful representation, the power density, when defined, is usually an approximation or average power density for a discharge corresponding to the ‘service time’ [2].

Ragone plots are intended to show the relationship between energy and power density [2]. Average powers from constant current discharges are commonly used and, often, the criteria are undefined [2]. Typically, cell capacities as a function of low power discharges are plotted. Different technologies are commonly compared on Ragone plots, presenting only a single data point or small shaded region for each technology.

Takei et al. used a constant power pulse method to determine rate capabilities of Li-ion batteries [3]. A constant power pulse is applied for either 30 s or until the cell reaches a lower cutoff voltage, which they define as 2.5 V (the same voltage as the OCV of a fully discharged commercial Li-ion cell). The cell is allowed to relax for 15 min and is then given another discharge pulse. From this data, they generated a plot of specific power vs. percentage DOD for various times (10, 20, and 30 s). Although their representation was more informative than a single-value

^{*} Corresponding author

power density, the regime which they studied was limited to a maximum of 500 W/kg [3].

We show that power density for secondary batteries cannot be faithfully represented by a single number, but must be represented as a function of the time scale for which the power can be delivered. In order to achieve this, the instantaneous specific power density (in W/kg) for various current discharges are plotted vs. time on the same graph. The line which connects the highest instantaneous power at any time is referred to as the Specific Power Profile (SPP) and empirically represents the largest power density which a cell can provide at any given time.

2. Experimental

Cells were cycled using a computer-controlled charger system. Power density was measured by discharging cells at a constant current using a Kikusui PLZ-700W electronic load.

Co Li-ion (Moli, 41 g, 1.5 A h, 18650-size), Mn Li-ion (Moli, 42 g, 1.35 A h, 18650-size), Ni–Cad (from cordless drill battery pack, 53 g, 1.6 A h, 22410-size), and Ni–MeH (from cordless drill battery pack, 55 g, 2.2 A h, 22410-size) cells were tested.

To separate the effects of self-heating, a few ‘isothermal’ discharges were performed on Mn Li-ion cells.

3. Results and discussion

As described above, if one chooses a lower cutoff voltage and a time limit, it is possible to arrive at a number

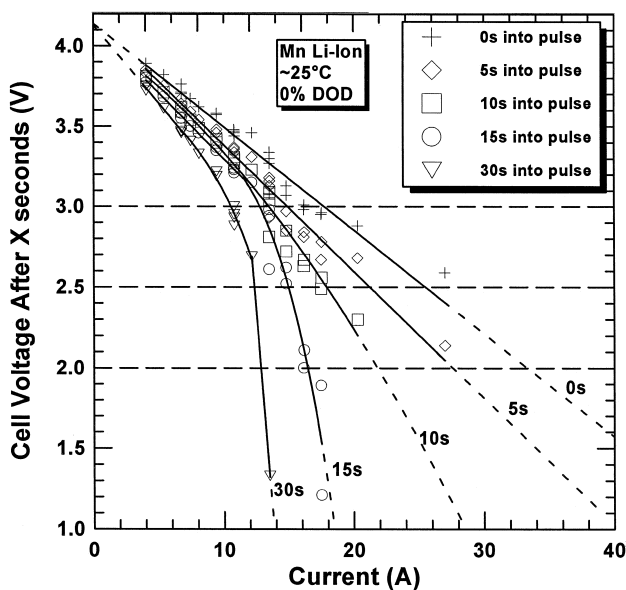


Fig. 1. Cell voltages 0, 5, 10, 15, and 30 s after start of discharge pulse. The data has been fit empirically with 1st, 2nd, and 3rd-order polynomials.

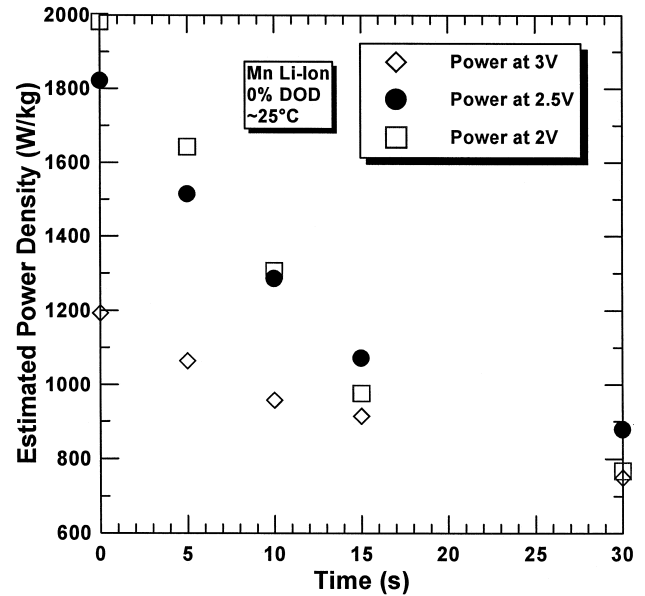


Fig. 2. Power densities calculated from the extrapolated and interpolated voltages shown in Fig. 1 using Eq. (2) plotted vs. time.

with units of power density. For illustrative purposes, we will begin by analyzing our Mn Li-ion cell data in this manner. The voltage recorded at a specific time, t , during discharge is plotted as a function of discharge current. If the data is roughly linear, it can then be fit and extrapolated to find the applied current which corresponds to some pre-determined lower cutoff voltage at time t . Fig. 1 shows an example of this type of plot (for fully charged Mn Li-ion cells), with data shown for $t = 0, 5, 10, 15,$ and 30 s. The first point measured after the start of the discharge is set as ‘0 s’. One can see that for $t > 5$ s, the curve becomes nonlinear, making extrapolation to higher currents unreliable. A power in watts per kilogram can then be defined by finding I_{LCV} such that:

$$V(I_{LCV}, t) = V_{LCV}, \quad (1)$$

where V_{LCV} is the cutoff voltage in volts (either 3.0, 2.5, or 2.0 V in this case), I_{LCV} is the current in amperes where the fit lines intersect at V_{LCV} . The power is then calculated using:

$$\text{Power density} = V_{LCV} \times I_{LCV} / M_{CELL}, \quad (2)$$

where M_{CELL} is the cell mass in kilograms.

Fig. 2 summarizes the power densities calculated by this method at each of these intersections by plotting the power densities (calculated using Eq. (2)) vs. time for V_{LCV} of 3.0, 2.5, and 2.0 V. Note that using this methodology, a very wide range of power densities can be attributed to the same cell design, depending on how one chooses voltage and time cutoffs. Using only one of these points to represent the power density of the cell is far too limiting and could be misleading.

Any choice of voltage limits or pulse time cannot generally be relevant to all applications. Fig. 2 also shows

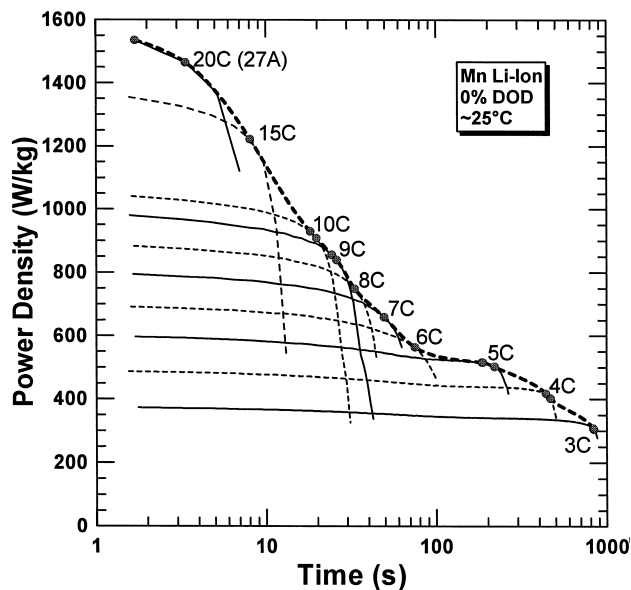


Fig. 3. The instantaneous power density plotted vs. time for many discharges of various currents. The thicker dashed line is, empirically, the highest power density which the cell can supply for the given length of time. We call this the Specific Power Profile (SPP).

that the choice of lower cutoff voltage (for Mn Li-ion cells) only has significant impact at times less than 15 s. Even then, the only significant difference is when V_{LCV} is chosen to be greater than the manufacturer's specification of 2.5 V. Therefore, it is the pulse duration which is the single most important factor in determining the derived power density. Therefore, a realistic representation of power density must include the pulse time dependence.

Fig. 3 shows plots of the instantaneous power output vs. time of fully charged Mn Li-ion cells discharged at various constant currents. The power density is calculated from the measured voltage and the electronic load set current, using a cell mass of 42 g. An additional line is plotted on this graph which connects up the highest measured powers as a function of time. This line is a purely empirical guide for the eye. We call it the Specific Power Profile (SPP). The SPP appears similar to Fig. 2. The SPP, however, is not calculated from arbitrarily set voltages. A more rigorous definition of the SPP will be provided below. What it represents is the highest power the cells can provide after a given period of time *at constant current*. Many applications run at constant power, and the SPP places a *lower bound* on the time for which the cell can deliver a particular constant power level.

For example, from Fig. 3, we can see that for an application which requires constant current for 10 s, Mn Li-ion can be expected to deliver ~ 1140 W/kg at the end of 10 s, and the current would be just below 15C (20.25 A). For constant power application requiring 1000 W/kg, we see that Mn Li-ion will be able to deliver this power for *at least* 14 s.

We believe that the SPP is an informative way to compare different cell technologies. Fig. 4 illustrates this by comparing the SPP of fully charged Mn Li-ion cells to those of fully charged Co Li-ion, Ni-Cad, and Ni-MeH cells. The SPPs of Co Li-ion, Ni-Cad, and Ni-MeH are almost equivalent in the $50 \text{ s} < t < 100 \text{ s}$ range, but otherwise, Li-ion is superior. Note that for discharges which contribute to the SPP in that range, the Ni-Cad and Ni-MeH cells heated to $> 55^\circ\text{C}$ and $> 60^\circ\text{C}$, respectively, about 1 min after the discharges were stopped. Further, the SPPs for Ni-Cad and Ni-MeH cells are very similar up to ~ 50 s when the higher capacity of the Ni-MeH cells becomes evident. Also, Mn and Co Li-ion SPPs cross near $t \cong 300$ s. It is therefore clear that comparing single numbers for power densities of various technologies is prone to error.

For Mn Li-ion technology, the effect of state of charge is seen to be rather trivial. Fig. 5 shows the SPP from Fig. 3 plotted with the SPP for Mn Li-ion cells at 80% DOD. The SPP is merely shifted downwards without changing shape. This is simply due to the lower average voltage of the cells. Only at time scales longer than 100 s does the reduced capacity of the cell have an effect on the SPP. The point of interest to the USABC criteria (30 s discharge from 80% DOD) [1] is marked with an open diamond (\diamond). The 'x' indicates the long-term USABC goal, which is about 2/3 what the Mn Li-ion cell can supply. Note that the cell voltage at the open diamond is $> 3/4$ of the 80% DOD OCV (in excess of the USABC requirement of 2/3).

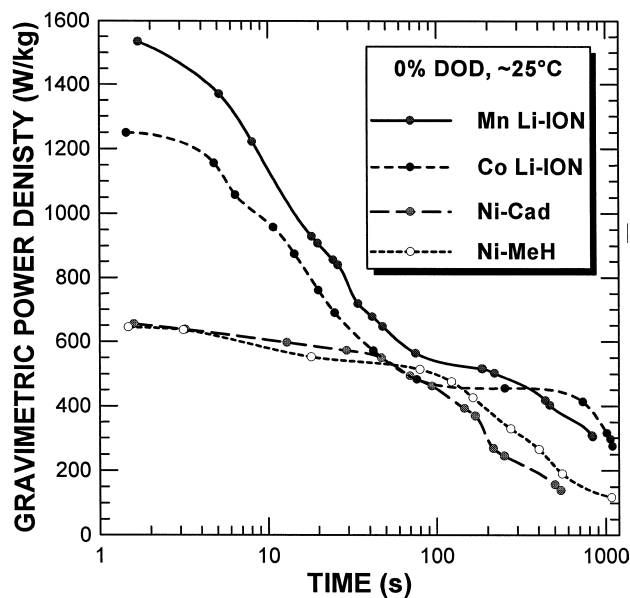


Fig. 4. Specific Power Profiles for fully charged manganese and cobalt cathode Li-ion and Ni-Cad cells. Note that the Ni-MeH and Ni-Cad cells self-heat to $> 55^\circ\text{C}$ and $> 65^\circ\text{C}$ for discharges contributing at ~ 80 s to the SPP.

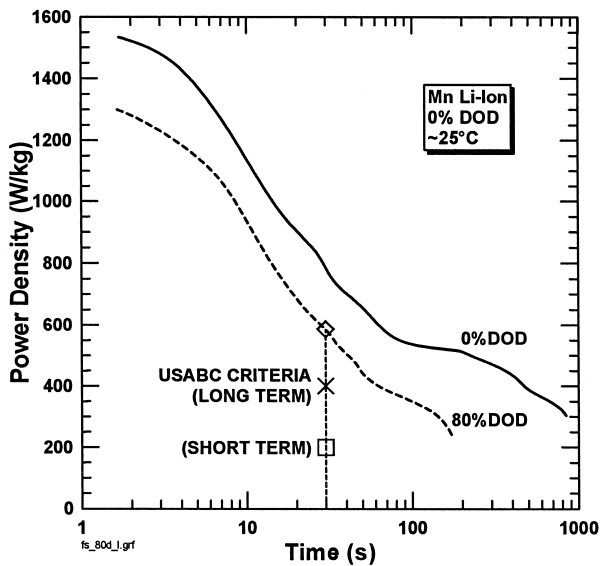


Fig. 5. Comparison of the SPP for fresh manganese cathode Li-ion cells at 0% and 80% DOD. The USABC long-term criteria is marked with an 'x'.

A more rigorous definition of the SPP is given by:

$$\text{SPP}(t, I) = \text{MAXIMUM OF } (I \times V(t, I) M_{\text{CELL}}) \text{ w.r.t. } I \quad (3)$$

Maximizing w.r.t. I at constant t is difficult, given that the data are usually collected at discrete times which will be different for each current. Interpolation techniques would be required.

There are many factors which contribute to the shape of the voltage curve. These include electrolyte depletion, electrode particle depletion, and cell capacity. Factors which affect the Li-ion diffusion rate include electrolyte

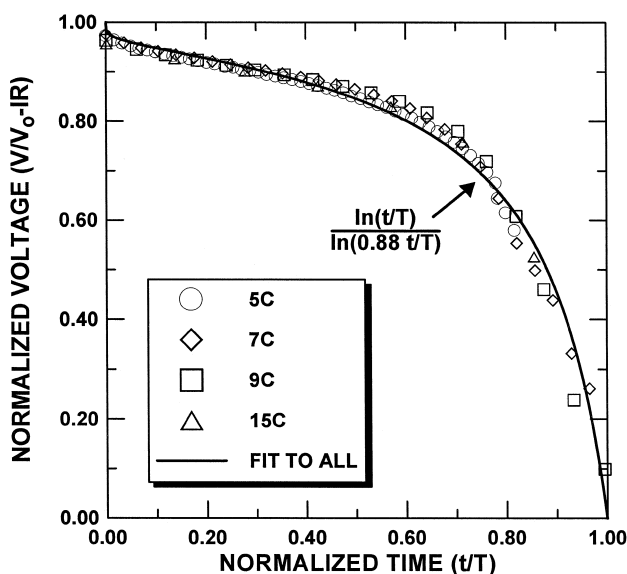


Fig. 6. The normalized voltage vs. the normalized time for 5°C, 7°C, 9°C, and 15°C isothermal discharges plotted with the fitted equation (T is a fitted normalization constant).

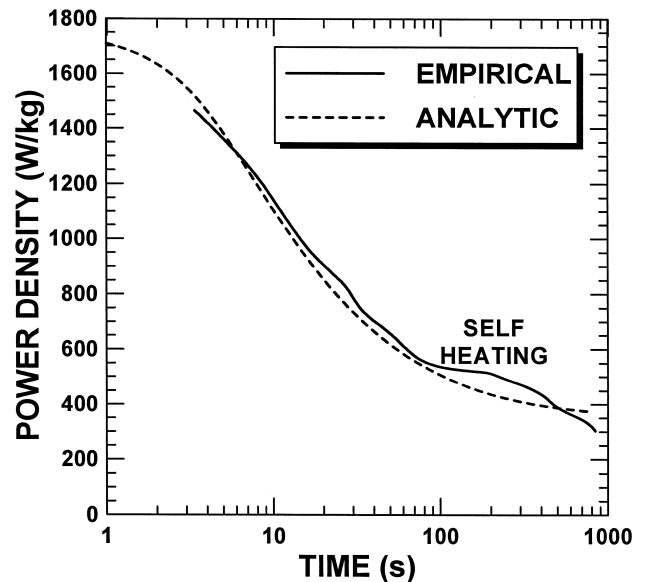


Fig. 7. Comparison of the analytic Mn Li-ion SPP (derived by fitting $V(t, I)$ to the discharges shown in Fig. 3 which did not self-heat significantly) and the empirical SPP for nonisothermal discharges. Note the deviation > 100 s due to self-heating.

composition, stack thickness, electrode porosity, and temperature. However, all the results which are dominated by depletion (i.e., not self-heating) will scale. By scaling the data, we can find an analytic form for $V(t, I)$ from which $\text{SPP}(t, I)$ can be accurately determined; the details of which will be the subject of another paper [4].

Several isothermal discharges were performed to increase our confidence that the analytic form of $V(t, I)$ is a general representation, valid over a wide range of currents. The normalized voltage profiles are shown in Fig. 6 with a fitted function.

Fig. 7 shows an analytic SPP plotted with the empirical SPP shown in Fig. 3. It was generated by fitting the analytic $V(t, I)$ to all the discharges shown in Fig. 3 which were dominated by electrolyte depletion, and did not show significant self-heating. By comparing them, we can see where the self-heating causes some deviation (> 100 s). Since the analytic $V(t, I)$ contains no information on the cell capacity or electrode particle surface depletion, the analytic SPP deviates again for times > 500 s.

4. Conclusions

Using single values to represent power densities is insufficient and potentially misleading. The commonly used representations of power density are not very informative for pulsed, high-power applications.

The SPP is an informative and well-defined representation of power density for the short-interval, high-power regime. All the values presented on the empirical SPP are measured (or interpolated) quantities. The SPP can be more rigorously defined by fitting (or modelling) the voltage profiles of the discharges.

References

- [1] United States Advanced Battery Consortium (USABC) Electric Vehicle Battery Test Procedures Manual, Revision 2, DOE/ID-10479, Rev. 2, January, 1996.
- [2] Various references in *The Handbook of Batteries and Fuel Cells*, 2nd edn., in: D. Linden (Ed.), McGraw-Hill, 1995.
- [3] K. Takei, Y. Kobayashi, M. Miyashiro, N. Terada, *Electrochem. Soc. Proc.* 97 (18) (1997) 382–388.
- [4] A.M. Wilson, Jan N. Reimers, to be submitted to the *Journal of the Electrochemical Society*.